JOURNAL OF AGRICULTURAL AND FOOD CHEMISTRY

Degradation of Cyanidin 3-Rutinoside in the Presence of (–)-Epicatechin and Litchi Pericarp Polyphenol Oxidase

LIANG LIU, SHAOQIAN CAO, BIJUN XIE,* ZHIDA SUN, AND JINJUN WU

College of Food Science and Technology, Huazhong Agricultural University, Wuhan, Hubei 430070, People's Republic of China

The degradation mechanism of cyanidin 3-rutinoside in the presence of (−)-epicatechin and litchi pericarp polyphenol oxidase (PPO) was investigated using several model systems. The enzymically generated (−)-epicatechin *o*-quinone could induce cyanidin 3-rutinoside degradation. The results obtained in this study allowed us to propose a pathway for cyanidin 3-rutinoside degradation in the presence of (−)-epicatechin and litchi pericarp PPO. First, enzymatic oxidation of (−)-epicatechin produced the corresponding *o*-quinone, and then cyanidin 3-rutinoside and (−)-epicatechin competed for (−)-epicatechin *o*-quinone, resulting in degradation of cyanidin 3-rutinoside and regeneration of (−)-epicatechin. Moreover, the results of kinetic studies indicated this competition was influenced by both (−)-epicatechin concentration and cyanidin 3-rutinoside concentration in the model system.

KEYWORDS: Cyanidin 3-rutinoside; polyphenol oxidase; litchi; (−)-epicatechin; degradation

INTRODUCTION

Litchi (*Litchi chinensis* Sonn.) is a subtropical fruit of high commercial value for its white, translucent aril and attractive red pericarp. Red color in litchi pericarp originates from the presence of anthocyanins which degraded rapidly during postharvest handling and storage. Degradation of anthocyanin causes tissue browning, which was thought to be attributed to the reactions catalyzed by polyphenol oxidase (PPO) (*1*–*3*). However, Jiang (*4*) reported that litchi PPO could not oxidize anthocyanins directly. Similar results were reported for grape PPO, blueberry PPO, and strawberry PPO (*5*–*7*).

Although anthocyanins were not direct substrates for PPO, anthocyanins were degraded rapidly by PPO in the presence of polyphenolic substrates (*5*, *6*, *8*–*11*). Wesche-Ebeling and Montgomery (*5*) reported that the presence of catechin increased the rate of degradation of strawberry anthocyanins by PPO. Cheynier et al. (*8*) confirmed enzymically generated *o*-quinines of caffeoyltartaric acid were involved in the degradation of anthocyanins. Sarni et al. (*6*) studied the degradation of cyanidin 3-glucoside and malvidin 3-glucoside in the presence of caffeoyltartaric acid and grape PPO. They suggested both anthocyanins reacted with the caffeoyltartaric acid *o*-quinone; cyanidin 3-glucoside was degraded mostly by coupled oxidation, whereas malvidin 3-glucoside formed adducts with caffeoyltartaric acid *o*-quinone. Karder et al. (*12*) reported cyanidin 3-glucoside was degraded by a coupled oxidation mechanism with integration of caffeic acid *o*-quinone into the degradation products.

Until now, the anthocyanins had been the most studied compounds in litchi pericarp, and cyanidin 3-rutinoside had been identified as the major anthocyanin in litchi pericarp (*3*, *13*). However, the mechanism of degradation of anthocyanin in litchi pericarp is still ambiguous. Moreover, as far as we know, there is no information available in the literature about degradation of anthocyanin by PPO in the presence of (−)-epicatechin, one of the major polyphenols in litchi pericarp (*13*). Thus, the purpose of this work was to investigate the anthocyanin degradation in the presence of litchi pericarp PPO and (−)-epicatechin using purified cyanidin 3-rutinoside.

MATERIALS AND METHODS

Plant Material. Fruit of litchi (*Litchi chinensis* Sonn. cv. Nuomici) at commercial maturation were obtained from Guangdong. The fruit arrived in the laboratory within 24 h of being harvested. Fruits were peeled, and the pericarp was stored at −30 °C until extraction.

Chemicals. (−)-Epicatechin was purchased from Sigma, and acetonitrile (HPLC-grade) was purchased from Fisher. All other chemicals were analytical-grade.

PPO Extraction. Litchi pericarp (100 g) was homogenized with 500 mL of acetone (−20 °C for 1 min), and the mixture was refrigerated for 2 h and then filtered (filtrate was used for anthocyanin purification). The residue was rinsed with 200 mL of acetone (−20 °C to eliminate phenolic compounds), and the PPO was in the residue. The residue was placed in the fume hood to remove the residual acetone, and acetone powder was obtained. Acetone powder of litchi was homogenized in 400 mL of 0.1 M phosphate buffer (pH 7.5) for 20 min, and then the homogenate was centrifuged at 8000*g* for 5 min. Solid ammonium sulfate was added to the supernatant; the precipitate obtained between 80 and 100% saturation was collected by centrifugation at 8000*g* for 10 min, and then the precipitate was dissolved in 0.1 M phosphate buffer (pH 7.8). The enzyme extract was dialyzed against the same buffer at 4 °C overnight.

* To whom correspondence should be addressed. Fax: +86-27-87282966. E-mail: bijunfoad@yahoo.com.cn.

10.1021/jf071931y CCC: $37.00
Published on Web 10/04/2007

Enzyme Activity and Protein Assay. PPO activity was assayed spectrophotometrically at 15 °C using (−)-epicatechin as the substrate by monitoring the sample at 385 nm. The reaction medium (3 mL) contained 1 mL of 3 mM (−)-epicatechin, 1.98 mL of 50 mM citrate buffer (pH 3.5), and 0.02 mL of the enzyme solution.

The protein content was determined according to Bradford's dye binding method, using bovine serum albumin (BSA) as a standard (*14*).

Isolation and Purification of Cyanidin 3-Rutinoside from Litchi Pericarp. The filtrate of acetone extract in the enzyme extraction process was concentrated under vacuum by a rotary evaporator at 40 °C. The concentration was loaded onto an XAD-16 Amberlite resin column [30 cm × 2.5 cm (inside diameter)], and the fraction eluted with an ethanol/water mixture (40:60, v/v) was collected. After ethanol had been removed, the fraction was extracted with ethyl acetate, and anthocyanins were in the water phase. Consequently, the anthocyanin fraction was applied on a Toyopearl HW-40S column [200 mm × 16 mm (inside diameter), Tosoh], and anthocyanins were eluted using a methanol/water/formic acid mixture (50:48:2, v/v) as the eluent at a flow rate of 0.8 mL/min. The major anthocyanin fraction was identified by reverse-phase high-performance liquid chromatography and mass spectrometry (RP-HPLC–MS).

RP-HPLC–MS Analyses. Selected samples were subjected to mass spectrometry analysis using an Agilent HPLC-MS system, which was equipped with an electrospray ionization (ESI) interface. The mobile phases consisted of (A) 2.5% (v/v) aqueous formic acid and (B) acetonitrile, water, and formic acid (57.5:40:2.5, v/v/v) and eluted with a flow rate of 0.2 mL/min. A ZORBAX Eclipse XDB-C18 column [4.6 mm × 150 mm (inside diameter), Agilent] was used, and a 2 μL sample solution was injected. The elution conditions were as follows: a linear gradient from 10 to 35% B over 25 min and from 35 to 100% B over 10 min, followed by washing and reconditioning of the column. The eluent was subsequently detected by ESI-MS in the positive ion mode. The orifice voltage was −30 V, and the heat capillary temperature was 325 °C. The mass scale was defined from *m*/*z* 100 to 1000.

Sugar Analysis. After hydrolysis of anthocyanin by heating at 100 °C for 60 min in 2 M HCl, the sugar residues were subjected to derivatization using the method described previously (*15*) and then determined by gas chromatography (GC). Briefly, the dry sugar residue and hydroxyamine hydrochloride were dissolved in 0.5 mL of pyridine without water and heated at 90 °C for 30 min. The reaction mixture was treated with 0.5 mL of acetic anhydride at 90 °C for 30 min and then was analyzed with a gas chromatograph which equipped with a flame ionization detector (280 °C) on a BP-21 capillary column [50 m × 0.32 mm (inside diameter), 0.32 μm] with helium as the carrier gas. The injector temperature was 280 °C, and the oven temperature started at 160 °C, then was increased at a rate of 10 °C/min to 180 °C, increased at a rate of 3 °C/min to 208 °C, and increased at a rate of 1 °C/min to 210 °C, and was held for 4 min. The injection volume was 1 μL in the split mode (50:1).

Reactions of PPO with (−)-Epicatechin and Cyanidin 3-Rutinoside. The reaction of PPO with (−)-epicatechin in combination with cyanidin 3-rutinoside was observed through continuous scanning from 300 to 600 nm using a SHIMADZU UV-1700 spectrophotometer at 15 °C. The assay medium (3 mL) contained (−)-epicatechin, litchi pericarp PPO, and cyanidin 3-rutinoside in 50 mM citrate buffer (pH 3.5). Effects of enzyme concentration, (−)-epicatechin concentration, and anthocyanin concentration on the rate of anthocyanin degradation were determined.

Statistical Analysis. For the measurement of the anthocyanin degradation rate and the (−)-epicatechin oxidation rate, each sample was assayed in triplicate. Means were compared using Tukey test with a $P < 0.05$ significance level.

RESULTS AND DISCUSSION

Purification and Identification of Cyanidin 3-Rutinoside from Litchi Pericarp. Cyanidin 3-rutinoside in litchi pericarp was purified with a Toyopearl HW-40S column and then identified by HPLC–ESI-MS. The ESI-MS spectrum of this anthocyanin recorded in the positive ion mode showed a signal with a molecular ion ($[M]^+$) at *m*/*z* 595. In the MS/MS spectrum, two fragment ions were detected at *m*/*z* 449 and 287. These data were in agreement with the data for cyanidin 3-rutinoside described by Sarni-manchado et al. (*13*), who suggested that the fragment ion at *m*/*z* 449 corresponding to the elimination of a rhamnosyl moiety from the anthocyanin and another fragment ion at *m*/*z* 287 corresponding to the cleavage of a hexosyl moiety from the glycosylated cyanidin. Sugar residue analysis demonstrated that residues of this anthocyanin were glucose and rhamnose, confirming the anthocyanin purified with a Toyopearl HW-40S column from litchi pericarp was cyanidin 3-rutinoside. Thus, this fraction of anthocyanin was used to investigate degradation of cyanidin 3-rutinoside by PPO in the presence of (−)-epicatechin.

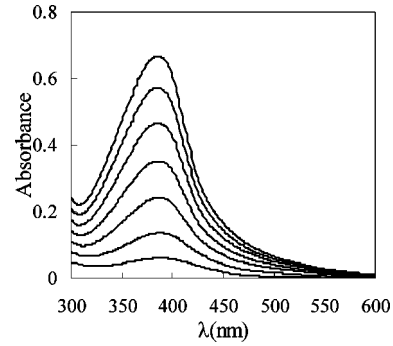

Figure 1. UV–vis spectra of a reaction solution of (−)-epicatechin and litchi pericarp PPO at pH 3.5. The assay medium (3 mL) contained 1 mM epicatechin and 1.8 μg of litchi pericarp PPO in 50 mM citrate buffer (pH 3.5). Scanning was carried out at 10 min intervals for 70 min.

Oxidation of (−)-Epicatechin by Litchi Pericarp PPO. Since there is little information available in the literature about the study of oxidation of (−)-epicatechin by PPO, oxidation of (−)-epicatechin by litchi pericarp PPO was investigated first. The spectrum of (−)-epicatechin oxidation showed a maximum absorption at 385 nm (**Figure 1**). This wavelength was similar to that of dehydrodicatechin A, which was a product of oxidation of (+)-catechin by either polyphenol oxidase or peroxidase (*16*, *17*), suggesting that the absorption at this wavelength might be due to the formation of dehydrodiepicatechin A, one isomer of dehydrodicatechin A. According to the (+)-catechin oxidation mechanism proposed by Guyot et al. (*18*), we presumed this compound was probably formed from the reaction between (−)-epicatechin and (−)-epicatechin *o*-quinone. Thus, we proposed a pathway of oxidation of (−)-epicatechin by PPO at pH 3.5, according to which (−)-epicatechin was oxidized to (−)-epicatechin *o*-quinone (reaction 1), and then *o*-quinone suffered the nucleophilic attack of (−)-epicatechin to form dehydrodiepicatechin A (reaction 2).

(111111111) (−)-epicatechin + PPO → (−)-epicatechin *o*-quinone (1)

(−)-epicatechin *o*-quinone + (−)-epicatechin → dehydrodiepicatechin A (2)

Degradation of Cyanidin 3-Rutinoside by PPO in the Presence of (−)-Epicatechin. A model system (3 mL) that contained 2.7 mM epicatechin, 1.8 μg of litchi pericarp PPO, and 0.18 mM cyanidin 3-rutinoside in 50 mM citrate buffer (pH 3.5) was monitored via spectroscopy between 300 and 600 nm, and the spectrum was recorded at 10 min intervals. The absorbance at 520 nm of cyanidin 3-rutinoside remained constant after incubation for 1 h in the absence of either PPO or (−)-epicatechin, indicating that no degradation of cyanidin 3-ruti-

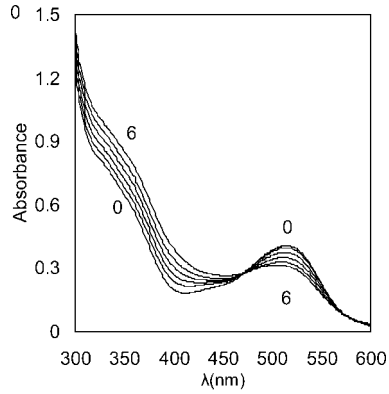

Figure 2. Spectrophotometric recordings for the degradation of cyanidin 3-rutinoside in the presence of (−)-epicatechin and litchi pericarp PPO, at 15 °C, in 50 mM citrate buffer (pH 3.5). The model system (3 mL) contained 2.7 mM epicatechin, 1.8 μg of litchi pericarp PPO, and 0.18 mM cyanidin 3-rutinoside in 50 mM citrate buffer (pH 3.5). Recordings 0–6 were scanned every 10 min from the beginning of the reaction.

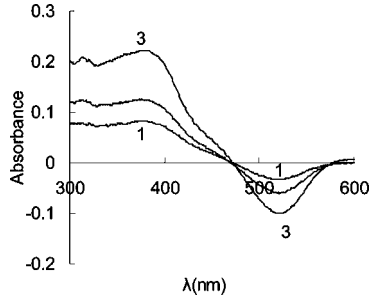

Figure 3. Changes in absorbance of the model system at different wavelengths during the reaction process. The model system (3 mL) contained 2.7 mM epicatechin, 1.8 μg of litchi pericarp PPO, and 0.18 mM cyanidin 3-rutinoside in 50 mM citrate buffer (pH 3.5). Plots 1–3 were determined 20, 30, and 60 min after the beginning of the reaction, respectively.

noside occurred and confirming anthocyanins were not direct substrates for litchi pericarp PPO (*4*).

In the presence of both PPO and (−)-epicatechin, the cyanidin 3-rutinoside concentration decreased rapidly. The absorbance between 480 and 550 nm decreased, while the absorbance between 300 and 450 nm increased (**Figure 2**). This was probably attributed to the degradation of anthocyanin pigment and the oxidation of (−)-epicatechin in the model system. We also observed a blue shift phenomenon for the maximal absorbance wavelength of the model system (**Figure 2**). This might be due to the fact that some products formed during the reaction process.

During the reaction process, we noticed that the absorbance at 520 nm decreased mostly while the absorbance at 385 nm increased mostly (**Figure 3**), indicating degradation of anthocyanin and formation of dehydrodiepicatechin A were two main reactions in the model system. In the first 5 min, the decrease in cyanidin 3-rutinoside concentration was unconspicuous, whereas the increase in absorbance at 385 nm was obvious (**Figure 4**). Afterward, the cyanidin 3-rutinoside concentration decreased rapidly and linearly. This indicated that the formation of dehydrodiepicatechin A was favored by this model system and anthocyanin degradation could occur only after an excess of *o*-quinone formed.

In this model system, we also observed that the oxidation rate of (−)-epicatechin was 3.0×10^{-3} OD/min, which was lower than that observed in the oxidation of (−)-epicatechin

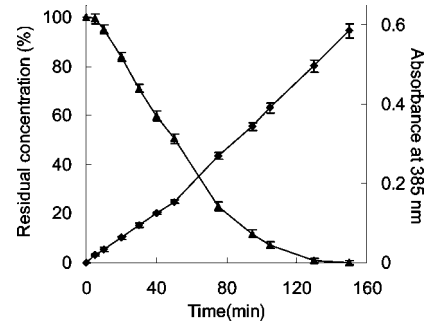

Figure 4. Degradation of cyanidin 3-rutinoside (▲) and formation of dehydrodiepicatechin A (◆) in the model system. The model system (3 mL) contained 2.7 mM epicatechin, 1.8 μg of litchi pericarp PPO, and 0.18 mM cyanidin 3-rutinoside in 50 mM citrate buffer (pH 3.5). Vertical bars indicate standard deviations of the mean.

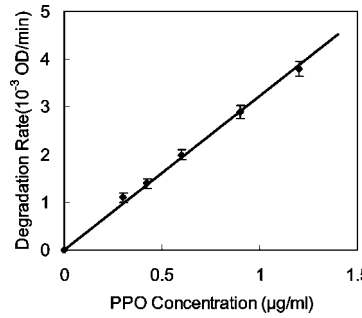

Figure 5. Effect of enzyme concentration on anthocyanin degradation. The model system (3 mL) contained 1.5 mM epicatechin, 0.18 mM cyanidin 3-rutinoside, and different PPO concentrations in 50 mM citrate buffer (pH 3.5). Vertical bars indicate standard deviations of the mean.

alone by litchi pericarp PPO (20.2×10^{-3} OD/min). This was probably due to the competition between (−)-epicatechin and anthocyanins for (–)-epicatechin *o*-quinone, which resulted in partial regeneration of (−)-epicatechin from its *o*-quinone by coupled oxidation of cyanidin 3-rutinoside (reaction 3). Similar results could be observed in cyanidin 3-glucoside-coupled oxidation by enzymically generated caffeoyltartaric acid *o*-quinone or chlorogenic acid *o*-quinone (*6–8*).

(−)-epicatechin *o*-quinone + cyanidin 3-rutinoside → (−)-epicatechin + cyanidin 3-rutinoside *o*-quinone (3)

After reaction for 50 min, the degradation rate of anthocyanin became slower, whereas the oxidation rate of (−)-epicatechin became faster (**Figure 4**). This further suggested the existence of some competition between (−)-epicatechin and anthocyanins for (−)-epicatechin *o*-quinone. However, the rate of oxidation of (−)-epicatechin did not increase after anthocyanin disappeared from the model system. This may be attributed to the inhibition of some oxidation products.

Kinetic Studies of Degradation of Cyanidin 3-Rutinoside by PPO in the Presence of (−)-Epicatechin. In accordance with the results described above, a coupled oxidation mechanism could be postulated. According to this mechanism, both anthocyanin and (−)-epicatechin competed for (−)-epicatechin *o*-quinone, resulting in degradation of cyanidin 3-rutinoside and regeneration of (−)-epicatechin. Therefore, we investigated the effects of enzyme, (−)-epicatechin, and anthocyanin concentrations on cyanidin 3-rutinoside degradation to confirm the coupled oxidation mechanism described above.

The relationship between the rate of cyanidin 3-rutinoside degradation and enzyme concentration is shown in **Figure 5**. Doubling the enzyme concentration would double the rate of

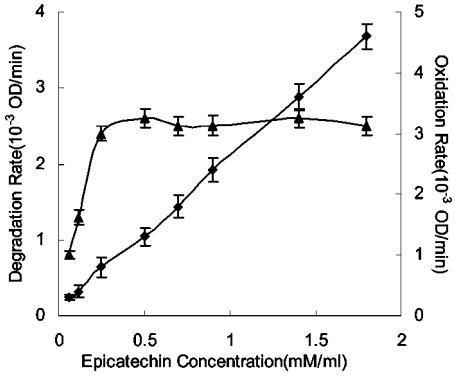

Figure 6. Effect of epicatechin concentration on anthocyanin degradation (▲) and epicatechin oxidation (◆) in the model system. The model system (3 mL) contained 1.8 μg of litchi pericarp PPO, 0.18 mM cyanidin 3-rutinoside, and different epicatechin concentrations in 50 mM citrate buffer (pH 3.5). Vertical bars indicate standard deviations of the mean.

cyanidin 3-rutinoside degradation. This could be easily explained by the fact that the increase in enzyme concentration accelerated the formation of *o*-quinone, resulting in the increase in the rate of anthocyanin degradation (*7*).

With fixed enzyme and anthocyanin concentrations, increasing the (–)-epicatechin concentration would have no significant effect ($P > 0.05$) on the rate of anthocyanin degradation when the (−)-epicatechin concentration was greater than 0.25 mM (**Figure 6**). However, the rate of formation of dehydrodiepicatechin A increased with the (−)-epicatechin concentration in the whole assayed concentration range (**Figure 6**). This was probably due to the fact that the (−)-epicatechin concentration influenced the competition between anthocyanin and (−)-epicatechin for (−)-epicatechin *o*-quinone. Although increasing the (−)-epicatechin concentration accelerated the formation of (−)-epicatechin *o*-quinone, it also increased the likelihood of coupled oxidation between (−)-epicatechin and (−)-epicatechin *o*-quinone. Under these conditions, anthocyanin may act as an antioxidant which inhibited reaction 2 in the model system. However, as the (−)-epicatechin concentration was lower than 0.25 mM, increasing the (−)-epicatechin concentration resulted in an increase in the rate of anthocyanin degradation (**Figure 6**). This may be due to the low rate of (−)-epicatechin *o*-quinone formation under these conditions.

With fixed enzyme and (−)-epicatechin concentrations, increasing the anthocyanin concentration reduced the rate of formation of dehydrodiepicatechin A (**Figure 7**). This could confirm that anthocyanin inhibited reaction 2 in the model system. As more anthocyanin was added, the (−)-epicatechin *o*-quinone concentration was reduced, leading to the increase in the rate of anthocyanin degradation and the decrease in the rate of dehydrodiepicatechin A formation. When the anthocyanin concentration was further increased, the rate of anthocyanin degradation did not significantly increase ($P > 0.05$) and the rate of dehydrodiepicatechin A formation did not significantly decrease ($P > 0.05$) (**Figure 7**). However, increasing the anthocyanin concentration could not completely inhibit the oxidation of (−)-epicatechin. In the model system with a high anthocyanin concentration, only anthocyanin was degraded and no dehydrodiepicatechin A formed in the first 30 min (**Figure 8**), suggesting only reaction 1 and reaction 3 occurred in this period. However, after 30 min, the absorbance at 385 nm began to increase, meaning reaction 2 occurred. This might due to the fact that part of the available (−)-epicatechin *o*-quinone reacted with (−)-epicatechin when the anthocyanin concentration decreased.

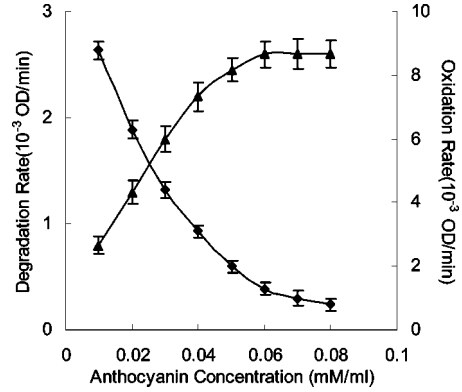

Figure 7. Effect of anthocyanin concentration on anthocyanin degradation (▲) and epicatechin oxidation (◆) in the model system. The model system (3 mL) contained 1.8 μg of litchi pericarp PPO, 1.5 mM epicatechin, and different cyanidin 3-rutinoside concentrations in 50 mM citrate buffer (pH 3.5). Vertical bars indicate standard deviations of the mean.

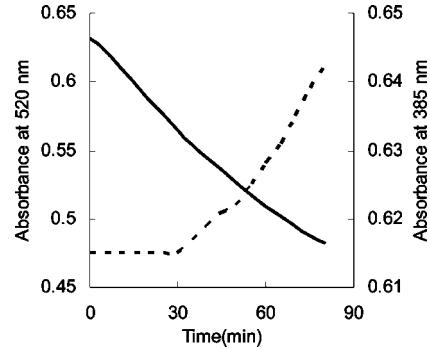

Figure 8. Degradation of cyanidin 3-rutinoside (—) and formation of dehydrodiepicatechin A (---) in the model system. The model system (3 mL) contained 1.5 mM epicatechin, 1.8 μg of litchi pericarp PPO, and 0.36 mM cyanidin 3-rutinoside in 50 mM citrate buffer (pH 3.5).

In conclusion, cyanidin 3-rutinoside was not degraded in the presence of litchi pericarp alone, but cyanidin 3-rutinoside could easily react with the enzymically generated (−)-epicatechin *o*-quinone, which led to the degradation of cyanidin 3-rutinoside. A pathway was proposed for cyanidin 3-rutinoside degradation in the presence of (−)-epicatechin and litchi pericarp PPO. First, enzymatic oxidation of (−)-epicatechin produced the corresponding *o*-quinone, and then cyanidin 3-rutinoside and (−)-epicatechin competed for (−)-epicatechin *o*-quinone, resulting in degradation of cyanidin 3-rutinoside and regeneration of (−)-epicatechin. Moreover, this competition was influenced by both (−)-epicatechin concentration and cyanidin 3-rutinoside concentration. However, HPLC analysis should be further employed to confirm the mechanism of coupled oxidation of anthocyanins described above. Characterization of reaction products of the coupled oxidation and further investigation of (−)-epicatechin enzymatic oxidation would be helpful for understanding the mechanism of anthocyanin degradation in the presence of (−)-epicatechin and PPO.

ACKNOWLEDGMENT

We thank Zhihong Xu of the Institute of Agricultural Biology and Technology of Guangdong for providing litchi fruit.

LITERATURE CITED

(1) Akamine, E. K. Preventing the darkening of fresh lychees prepared for transport. *Hawaii, Agric. Exp. Stn., Tech. Prog. Rep.* **1960**, *127*, 3–17.

(2) Huang, P. Y.; Hart, H.; Lee, H.; Wicker, L. Enzymatic and color changes during postharvest storage of lychee fruit. *J. Food Sci.* **1990**, *55*, 1762–1763.
(3) Lee, H. S.; Wicker, L. Anthocyanin pigments in the skin of lychee fruit. *J. Food Sci.* **1991**, *56*, 466–483.
(4) Jiang, Y. M. Role of anthocyanins, polyphenol oxidase and phenols in lychee pericarp browning. *J. Sci. Food Agric.* **2000**, *80*, 305–310.
(5) Wesche-Ebeling, P.; Montgomery, M. W. Strawberry polyphenoloxidase: Its role in anthocyanin degradation. *J. Food Sci.* **1990**, *55*, 731–734.
(6) Sarni, P.; Fulcrand, H.; Souillol, V.; Souquet, J. M.; Cheynier, V. Mechanisms of anthocyanin degradation in grape must-like model solutions. *J. Sci. Food Agric.* **1995**, *69*, 385–391.
(7) Kader, F.; Haluk, J.-P.; Nicolas, J.-P.; Metche, M. Degradation of cyanidin 3-glucoside by blueberry polyphenol oxidase: Kinetic studies and mechanisms. *J. Agric. Food Chem.* **1998**, *46*, 3060–3065.
(8) Cheynier, V.; Souquet, J. M.; Kontek, A.; Moutounet, M. Anthocyanin degradation in oxidising grape musts. *J. Sci. Food Agric.* **1994**, *66*, 283–288.
(9) Kader, F.; Rovel, B.; Girardin, M.; Metche, M. Mechanism of browning in fresh highbush blueberry fruit (*Vaccinium corymbosm* L). Role of blueberry polyphenol oxidase, chlorogenic acid and anthocyanins. *J. Sci. Food Agric.* **1997**, *74*, 31–34.
(10) Sarni-Manchado, P.; Moutounet, M. Reactions of polyphenoloxidase generated caftaric acid o-quinone with malvidin 3-o-glucoside. *Phytochemistry* **1997**, *45*, 1365–1369.
(11) Kader, F.; Irmouli, M.; Nicolas, J. P.; Metche, M. Proposed mechanism for the degradation of pelargonidin 3-glucoside by caffeic acid o-quinone. *Food Chem.* **2001**, *75*, 139–144.
(12) Kader, F.; Irmouli, M.; Zitouni, N.; Nicolas, J. P.; Metche, M. Degradation of cyanidin 3-glucoside by caffeic acid o-quinone. Determination of the stoichiometry and characterization of the degradation products. *J. Agric. Food Chem.* **1999**, *47*, 4625–4630.
(13) Sarni-manchado, P.; Erwan, L. R.; Guernevé, C. L.; Lozano, Y.; Cheynier, V. Phenolic composition of litchi fruit pericarp. *J. Agric. Food Chem.* **2000**, *48*, 5995–6002.
(14) Bradford, M. M. A rapid and sensitive method for the quantification of microgram quantities of proteins utilising the principle of protein-dye binding. *Anal. Biochem.* **1976**, *72*, 248–254.
(15) Zhang, W. J. *Biochemistry research technology of glycoconjugate*; Zhejiang University Publishing House: Hangzhou, China, 1999; pp 38–40.
(16) Lopez-Serrano, M.; Barcelo, A. R. Reversed-phase and size-exclusion chromatography as useful tools in the resolution of peroxidase-mediated (+)-catechin oxidation products. *J. Chromatogr., A* **2001**, *919*, 267–273.
(17) Guyot, S.; Cheynier, V.; Vercauteren, J. Structural determination of colourless and yellow dimers resulting from (+)-catechin coupling catalysed by grape polyphenoloxidase. *Phytochemistry* **1996**, *42*, 1279–1288.
(18) Guyot, S.; Cheynier, V.; Souquet, J. M.; Moutounet, M. Influence of pH on the enzymatic oxidation of (+)-catechin in model systems. *J. Agric. Food Chem.* **1995**, *43*, 2458–2462.

Received for review June 28, 2007. Revised manuscript received September 11, 2007. Accepted September 14, 2007.

JF071931Y